AIAA JOURNAL
Vol. 39, No. 11, November 2001

Probe Diagnostics of Gas Discharges in Supersonic Airflows

A. Ershov,* N. Ardelyan,† S. Chuvashev,† V. Shibkov,‡ and I. Timofeev‡
Moscow State University, 119899, Moscow, Russia

A new case of probe diagnostics of plasma density under the condition typical for plasma aerodynamic applications (high voltage and electric field, high nonequilibrium between components, high gas pressures, and a considerable compression effect) has been examined. The experiments have been carried out in dc and pulsed periodic discharges in supersonic airflows with Mach number $M = 2$ at the static ambient pressure range 10–200 torr. A personal-computer controlled double probe with an optogalvanic isolation based on an optocoupler and a fiber optical waveguide have been developed and tested in the gas discharges. A new theory of probe diagnostics of plasmas with a very high electric field in a supersonic airflow is developed based on a computer simulation of the interaction of the probe and the plasma flow. A combined effect of the flow compression and the electric field perturbation on the plasma density near the probe is revealed. This effect can limit the area of applicability of the probe diagnostics. Measures to prevent this negative effect are suggested. The results of probe diagnostics of the plasma density are in good agreement with those obtained using the microwave interferometer and the spectral method.

Introduction

THE study of characteristics of gas discharges in supersonic flows is of interest for the solution of such applied problems as the problem of fuel ignition in a hypersonic vehicle ramjet with supersonic combustion or the problem of reduction of drag of hypersonic vehicles. However, the parameters of dc discharges in a supersonic high-pressure airflow have been poorly investigated. In addition to the difficulties of creating such discharges, they are characterized by inhomogeneous and unsteady parameters.

Under these conditions, the main advantage of the probe method (the possibility of local measurements with a high temporal resolution) becomes important. However, application of standard schemes and methods of processing probe characteristics for such discharges is practically impossible due to the specific mode of operation of a probe in such discharges, which are characterized by a combination of several extreme conditions: high plasma potential ($V \geq 1$ kV), high discharge current ($I \geq 1$ A), large modulation of the discharge current and voltage, high gas pressure ($p \geq 10$ torr), a very high electric field ($E \geq 100$ V/cm) present in the discharge plasma, supersonic flow mode ($M \geq 1$), and chemical reactions (including ionization and recombination) in the air plasma.

The three first conditions create experimental difficulties of a probe characteristic measurement. However, there are difficulties of probe curve interpretation, even if its measurements are realized. The well-known theories of electrical probes in flows of high-pressure weakly ionized plasma are considered Refs. 1 and 2. However, the influence of the discharge electrical field, which provides the discharge current, on probe characteristics has always been ignored. Only in Ref. 3 has the limiting case of very high discharge electric fields been analyzed; however, only the electron branch of the probe curve has been considered, no ionization and recombination had been taken into account, and the plasma flow was far slower. The majority of research in case of supersonic plasma flow were carried out for wall probes. With the exception of Ref. 4, few works consider supersonic plasma flows leading to shock formation near the probe. However, in Ref. 4, no chemical reactions are present.

A new effort has proven to be needed because we do not know of any method for the correct interpretation of the probe measurements in terms of unperturbed plasma parameters.

Received 5 June 2000; revision received 10 November 2000; accepted for publication 9 April 2001.

*Associate Professor, Department of Physics.
†Professor, Department of Computer Science.
‡Professor, Department of Physics.

Experimental Setup

The experimental setup for development and testing of probe diagnostic methods is built around a stainless-steel cylindrical gas/vacuum chamber (Fig. 1). The chamber is 3 m long and about 1 m in diam. It consists of two sections that can form a vacuum-tight junction with the help of a lever-operated gate. The supersonic airflow was formed in the chamber by opening an electric valve and filling it with the atmospheric air through a converging–diverging nozzle with Mach number $M = 2$. The valve was driven by the power source synchronized with the discharge power supply. The flow duration was about 1.5 s. The cylindrical dielectric nozzle had a diameter of 15.4 mm critical cross section and an outlet diameter of 26 mm.

The experiments were carried out for the transversal dc and pulsed periodic (PP) discharges. The electrodes were placed in the supersonic airflow about 0.5–1 cm below the nozzle end. They were made of a stainless-steel rod, 3 mm in diam. Along 5 mm, their cross sections were ground from two sides to form an elliptic cylinder. The designs of the anode and the cathode were identical.

A controlled electric power source (voltage up to 5 kV, current up to 3 A) was used to drive the dc discharge. The PP discharges were fed by a power supply unit with voltage up to 24 kV, current up to 40 A, pulse duration 1–500 μs, repetition rate 1–1000 Hz, maximal pulsed power up to 1 MW, and average power consumption about 1 kW. The value of ballast resistance R_b was varied from 0.5 to 115 kΩ.

A shadow device was used for the supersonic airflow visualization. The electrical probes were used for a measurement of a plasma density, floating potential, and electric field in the plasma.

A personal-computer-controlled analyzer of optical spectra based on a spectrograph with inverse linear dispersion 0.35 nm/mm for the spectral region of 300–400 nm was used for registration of the plasma radiation spectra. The sensor of plasma radiation based on a charge-coupled device image sensor Toshiba TCD 1300D forms a video signal directly proportional to the radiation intensity in the spectral band 300–900 nm. The registration time for one frame was 20 ms. The measured spectra were used for determination of gas temperature and electron density.

For independent measurements of plasma electron density, a microwave ($\lambda = 8$ mm) interferometer was used. Double-beam pulsed storage oscilloscopes C8-17 with a 10-MHz passband and 1-mV/cm sensitivity were used for registration of the waveform of the discharge voltage and current, probe floating electric potential, and microwave interferometer signals.

Transversal DC Discharge in a Supersonic Airflow

Typical appearance of the transversal discharge in a supersonic gas flow (Fig. 2) is characterized by a formation of a couple of extended brightly radiating plasma channels, and of a less bright

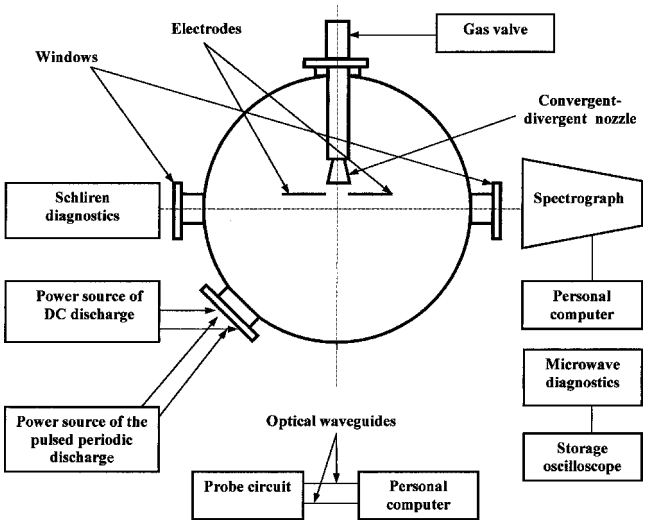

Fig. 1 Draft scheme of the experimental setup.

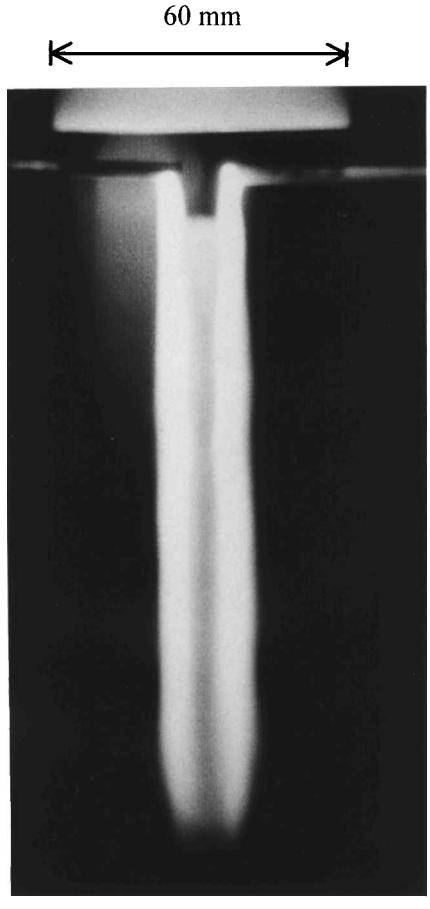

Fig. 2 Transversal dc discharge in the supersonic airflow: $P = 40$ torr, $I = 1.3$ A, and $M = 2$.

zone between them. The channels begin on the electrodes, and they are positioned in a direction parallel to the stream.

The scale of Fig. 2 is the external diameter of the nozzle, which is equal to 60 mm. Thus, the length of the discharge in Fig. 2 is equal to about 130 mm.

The registrations of the discharge current and voltage waveform (Fig. 3) have shown that these curves have a brightly expressed pulsing character with a frequency from 1 to 50 kHz. The oscillation frequency depends on external parameters of the discharge. The dependencies of the frequency on flow velocity and electrode separation are the strongest. The discharge in a supersonic airflow is characterized with high values of discharge voltage. As an example, the voltage of discharge with the interelectrode separation about 1 cm achieved a magnitude about 3 kV at a low current in our experiments.

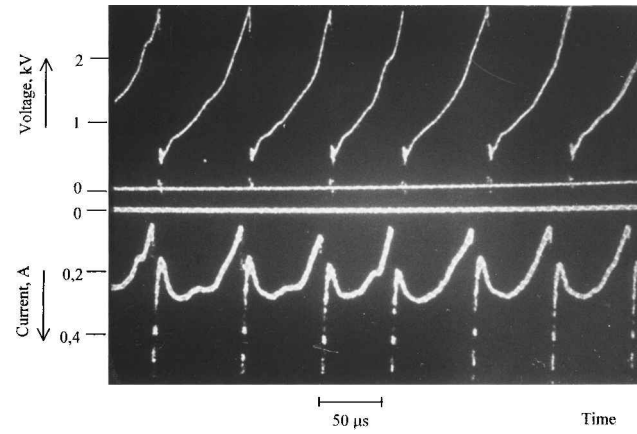

Fig. 3 Oscillograms of voltage and current of a dc discharge in supersonic airflow at $P = 40$ torr and $M = 2$.

Similar oscillations are typical not only of the dc discharge, but also for the PP discharge, when the pulse duration begins to exceed a certain magnitude. Thus, the oscillations of the discharge current and voltages are basic features of the discharge in supersonic airflow.

Our experimental and theoretical research[5] has shown that zones with a high ionization rate are formed near the anode and cathode, in which the electrical field (which provides, in particular, the movement of ions to the cathode opposite in direction to supersonic flow) is very high. The area with a rather weak field, which provides the electric current connection between these zones, is similar to a positive column. The positive column of a transversal dc discharge is always swept down by a flow with a speed equal to that of the flow; as a consequence, its length grows continuously. Therefore, at a given discharge current, the voltage between the cathode and anode also grows. As the voltage increases sufficiently, it initiates a new breakdown between the cathode and anode and forms a new positive column. The new column resistance is much less than that of an old column due to the smaller length. Therefore, after the breakdown, the discharge current flows in a new positive column. This new positive column also is swept down, while the old one is disintegrated. Then the breakdown process is repeated. Therefore, the discharge is not as homogeneous as one could conclude from its time-integrated appearance in Fig. 2, which had been taken with an exposure of $\frac{1}{60}$ s. Thus, an electrode discharge in a supersonic airflow is, as a rule, inhomogeneous and nonstationary.

Probe Design and Measurement Circuit

A double probe seems to be the optimal choice for the conditions just described. In such a case, both probe surfaces always have a negative potential reference to the local plasma potential, and the probe current is always limited by the ion saturation current. If the probes are both placed in the same equipotential surface of the plasma, the voltage between them is (in a certain approximation) independent of the local potential fluctuation.

The probe sizes and geometry were defined by our computer simulation of the environment around the probe (to be discussed). Our computer simulation has shown a rarefaction of the gas and an enhancement in the electric field near the probe surface. The calculation has also shown that a multiple growth of the local plasma characteristic parameter E/n_g, intensive ionization, and multiple rise in plasma density can result, and, thus, can bring a considerable growth in the probe current. No inferring of the unperturbed plasma density is possible in this case. Therefore, it is desirable to decrease the probe radius. However, to reduce these effects, the probe is to be mechanically stable in the flow and to endure high temperature. A compromise between these factors has resulted in the construction

of a double cylindrical probe with a diameter of 0.2–0.5 mm and length of 2–4 mm, made of Mo or W wires and placed inside an Al_2O_3 capillary.

A mechanical system has been used for a precise positioning of the probes in the discharge region. The probe can be slowly moved both in the vertical and in the horizontal planes by two electric motors. The mechanical system is installed inside the work chamber. The control of its operation is carried out with a control desk that is placed outside the chamber. It is joined with the mechanical system through a hermetic connection.

The double probe was positioned in brightly radiating plasma channels behind the cathode or anode. The plane of the double probe was oriented with respect to the direction of a flow. The angle was determined by a ratio of longitudinal and transversal components of the electric field of discharge (discussed later). Such an orientation ensured the disposition of the probes in an equipotential plane of the discharge.

Two types of electric circuits were developed and tested. The first type consists of two blocks: a probe unit, which was joined to the probe, and a measuring unit, which was fed to the computer. The blocks were connected with a long (100-m) optical waveguide. Both measurement and control signals were transferred through the waveguide. A circuit with a discharging capacitor was used to measure the probe characteristic.[6] The optical signal generated in the probe unit was proportional to the probe current. The signal was transmitted to the control unit where the inverse conversion and digitizing of the signal were carried out. The transfer linearity was checked by a special test, which was carried out before the beginning of the measurement. The test uses the same circuit with a known resistor instead of the probe. In one mode of operation, the polarity of the voltage between the two probes was changed to the opposite, after a measurement of one branch of the voltage–current characteristic of the double probe, and then the second branch was measured; the whole process was repeated. In the other mode, only one branch was measured several times.

The second type of the circuit consists of a single block, the optical output is formed with an optocoupler, and the exchange of signals with the computer is carried out through a 10-m-long standard computer cable. The voltage between the probes at the measurement of the probe characteristics was changed stepwise by the computer.

The time of a cycle of a measurement of one point of probe voltage–current characteristic was equal to $\approx 10\,\mu$s in both cases.

Development of a Theoretical Background of Probe Diagnostics for Plasma Aerodynamics: Numerical Simulation

The flowing plasma–probe interaction is described by the fluid equations for a neutral ($n_i = n_e$) plasma in the local diffusional approximation:

$$\frac{\partial \rho_g}{\partial t} + \operatorname{div}(\rho_g \boldsymbol{v}_g) = 0, \qquad \frac{\rho_g \, \mathrm{d}\boldsymbol{v}_g}{\mathrm{d}t} = -\operatorname{grad} p_g$$

$$\frac{\rho_g \, \mathrm{d}\varepsilon_g}{\mathrm{d}t} = -p_g \operatorname{div} \boldsymbol{v}_g, \qquad \frac{p_g}{\rho_g \varepsilon_g} = \gamma - 1, \qquad p_g = \frac{\rho_g k_B T_g}{m_{\mathrm{mol}}} \tag{1}$$

$$\operatorname{rot} \boldsymbol{E} = -\frac{\partial \boldsymbol{B}}{\partial t}, \qquad \operatorname{rot} \boldsymbol{B} = \mu_0 \boldsymbol{j}, \qquad \operatorname{div} \boldsymbol{B} = 0, \qquad \boldsymbol{j} = \sigma \boldsymbol{E}$$

$$\sigma = e n_e \mu_e, \qquad \frac{\partial n_i}{\partial t} + \operatorname{div}(n_i \boldsymbol{v}_i) = K_I - K_{DR}$$

$$\boldsymbol{v}_i = \boldsymbol{v}_g + \mu_i \boldsymbol{E} - \operatorname{grad}(D_a n_i), \qquad -\operatorname{div} \lambda_e \operatorname{grad} T_e + S_F - S_e = 0$$

For the numerical simulation, the electrical field equations in a quasi-stationary approximation are used instead of those of Eq. (1):

$$\operatorname{div} \boldsymbol{j} = 0, \qquad \boldsymbol{j} = \sigma \boldsymbol{E}, \qquad \boldsymbol{E} = -\operatorname{grad} \varphi$$

where ρ_g, p_g, ε_g, T_g, and $\boldsymbol{v}_g$ are density, pressure, internal energy, temperature, and velocity of the neutral gas, γ is its adiabatic exponent, $\gamma = 1.4$, m_{mol} is the molecular mass, k_B is the Boltzmann constant, μ_e is the electron mobility,

$$\mu_e = e/(m_e \nu_e), \qquad \nu_e = n_g \Sigma_e (2eT_e/m_e)^{\frac{1}{2}} \tag{2}$$

Σ_e is the electron elastic scattering cross section, e and m_e are the electron charge and mass, $\Sigma_e \approx 0.8 \times 10^{-20} T_e^2 + 0.43 \times 10^{-19} T_e + 0.8 \times 10^{-19}$, where T_e is the electron temperature. $\boldsymbol{E}$ is the electric field, φ is its scalar potential, $\boldsymbol{B}$ is the magnetic field inductance, $\boldsymbol{v}_i$ is the ion drift velocity, μ_i is the ion mobility, and D_a is the ambipolar diffusion coefficient,

$$\mu_i = e/(m_{\mathrm{mol}} \nu_{\mathrm{im}}), \qquad D_a = D_i[1 + eT_e/(k_B T_g)]$$

$$D_i = k_B T_g/(\nu_{\mathrm{im}} m_{\mathrm{mol}}), \qquad \nu_{\mathrm{im}} = \Sigma_{\mathrm{im}} n_g (2k_B T_g/m_{\mathrm{mol}})^{\frac{1}{2}} \tag{3}$$

Σ_{im} is the ion–molecule scattering cross section, where $\Sigma_{\mathrm{im}} \approx 2.2 \times 10^{-18} + 0.338 \times 10^{-16}/T_g^{1/2} \cdot K_{DR}$, and K_I are the rates of (dissociative) recombination and ionization,

$$K_{DR} = n_e^2 \, 3.3 \times 10^{-14} \big/ T_e^{\frac{1}{2}}, \qquad K_I = \Phi n_i n_g \alpha$$

$$\log_{10}(\alpha) \approx -13.6(\log_{10} Te)^2 + 15.7 \log_{10} Te - 21.4 \tag{4}$$

The factor Φ takes into account the deviation of the electron distribution function from the Maxwell one due to ionization: The number of electrons with energies corresponding to high cross sections of the inelastic collisions is less than at equilibrium, and the number of such collisions is $1/\Phi$ times less. This deviation is a result of an intense loss of energy by electrons in the corresponding energy band. This factor can be estimated as

$$\Phi = \left[(1 + 4C_\phi)^{\frac{1}{2}} - 1\right] \Big/ \left[(1 + 4C_\Phi)^{\frac{1}{2}} + 1\right] \Big/ C_\Phi$$

$$C_\Phi = T_e \nu'_{ei}/(2\nu'_{ee} I_i)$$

$$\nu'_{ee} = n_e [2e(I_i + T_e)/m_e]^{\frac{1}{2}} \Sigma_{ee}, \qquad \nu'_{ei} = n_g [2e(I_i + T_e)/me]^{\frac{1}{2}} \Sigma_i$$

$$\Sigma_i \approx 10^{-19} T_e, \qquad \Sigma_{ee} = a_0^2 \, 64\pi (27.2/T_e)^2 \ell n \Lambda$$

$$\ell n \Lambda \approx 26 + 1.5 \log_{10}(T_e) - 0.5 \log_{10}(n_e) \tag{5}$$

where I_i is the ionization energy for the molecules, a_0 is the Bohr radius, and λ_e is heat conductivity,

$$\lambda_e = 5 \big/ 2e^2 T_e n_e \big/ (m_e \nu_e)$$

S_F is the power of the electron gas heating by the field, where $S_F = \sigma \boldsymbol{E}^2$, and S_{eV} is the power of its cooling by collisions with excitation of vibration:

$$S_{eV} = n_g n_e (2k_B T_e/m_e)^{\frac{1}{2}} \sigma_{01}$$

$$\times \exp(-h\nu_V/k_B T_e) \big/ [1 - \exp(-h\nu_V/k_B T_e)]^2 \tag{6}$$

here $h\nu_V$ is the vibration quantum, σ_{01} is a cross section of the first vibration energy level excitation, T_e is the electron temperature. S_e^* is the power of the electron gas cooling by collisions with excitation of electron states:

$$S_e^* = \Sigma_s n_{gs} n_e E_s^* \int \max\left[0, \frac{\Sigma_s^*\left(E - E_s^*\right)}{T_e}\right] \left(\frac{2E}{m_e}\right)^{\frac{1}{2}}$$

$$\times \exp\left(\frac{-E}{T_e}\right) \frac{\mathrm{d}E}{T_e} \tag{7}$$

Here the summation was performed for the excitation of oxygen and nitrogen, where $\boldsymbol{n}_{gs}$ are the corresponding gas concentrations, Σ_s^* is the cross section of excitation for electron energy $E = T_e + E_s^*$, where E_s^* is the threshold energy.

All of the used quantitative data are taken as recommended in Ref. 7. In the approximating formulas I_i, E, E_s^*, and T_e are in electron volts; the rest of the values are in the main SI units.

Boundary conditions for the fluid equations defined the parameters of the unperturbed plasma flow (T_{g0}, M_0, n_{i0} , p_{g0}, and T_{e0})

on one side, for example, the bottom side, and a free exit (zero normal gradients) on all of the other sides. The unperturbed electric field E_0 was defined by electric potentials $\varphi_1 = +E_0 L_0/2$ and $\varphi_2 = -E_0 L_0/2$ on opposite boundaries, for example, left and right sides, were L_0 is the size of the computation area. The boundaries were positioned far from the probe ($L_0 \gg R$; Fig. 4) to minimize the corresponding errors.

These equations were solved for a two-dimensional (planar) problem. This is a good approximation if the probe cylinder is sufficiently long and both the unperturbed discharge electric field $\boldsymbol{E}_0$ and the unperturbed plasma flow velocity $\boldsymbol{v}_0$ are positioned in a plane normal to the probe's axis. The free Lagrangian method based on completely conservative implicit difference schemes on adaptive triangular grids[8] was applied. The gas dynamic equations were solved separately (the neutral gas does not feel the presence of the weakly ionized plasma for the characteristic short time of presence of an element of mass in the perturbed area near the probe). Because a flow over a cylinder is unstable, the neutral gas flow computation was carried out until quasi-periodical formation of vortices was established. The rest of the equations were solved with use of frozen distributions of neutral gas parameters.

The accuracy of the numerical results is estimated to be about 30%, the main sources of errors are uncertainties in plasma properties and the assumptions of the model. The codes applied provide much higher accuracy of a mathematical problem solution. The conservation of energy, mass, and momentum was checked during the computations. Some results of these computations are presented in Figs. 5–8 for the conditions close to those in the corresponding

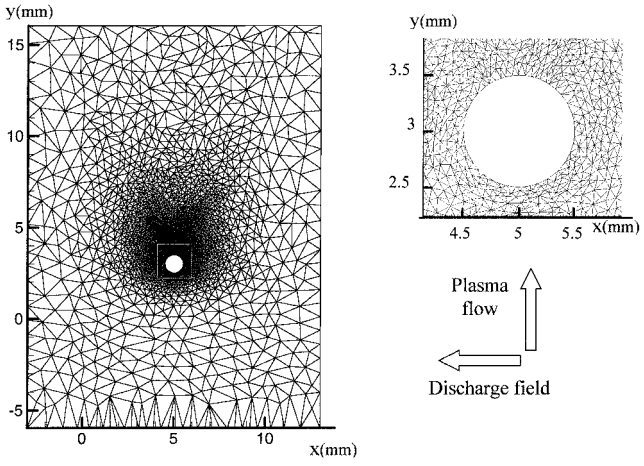

Fig. 4 Mesh for computer simulation of flow over a cylindrical probe.

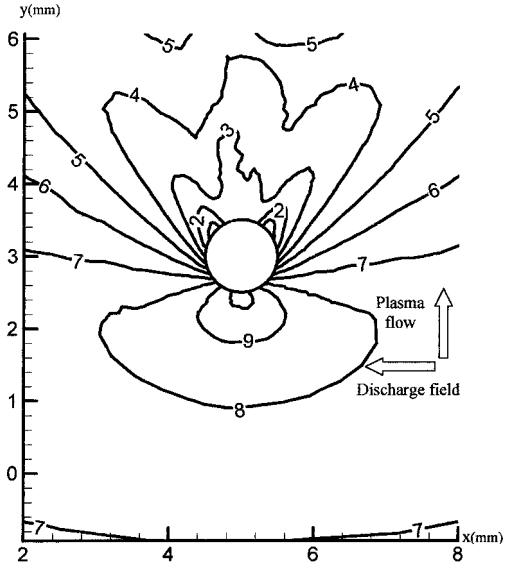

Fig. 5 Contour distribution of the gas density ($\times 10^{-18}$ cm^{-3}): 1, 0.15; 2, 0.25; 3, 0.35; 4, 0.45; 5, 0.55; 6, 0.65; 7, 0.75; 8, 0.85; 9, 0.95; and 10, 1.05.

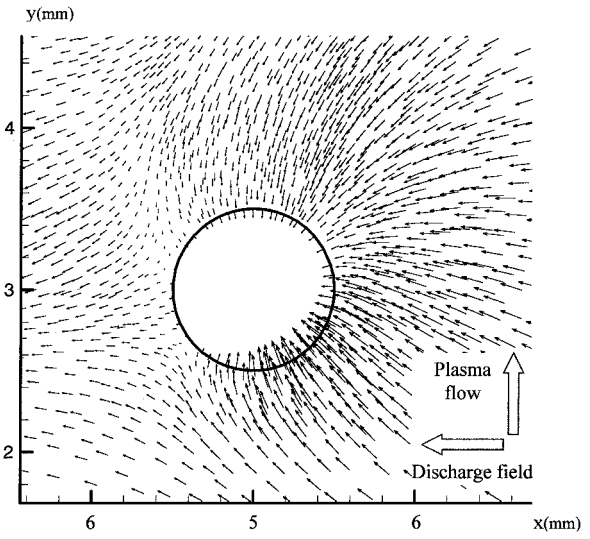

Fig. 6 Electric field distribution near the probe; unperturbed field in the far zone is 240 V/cm.

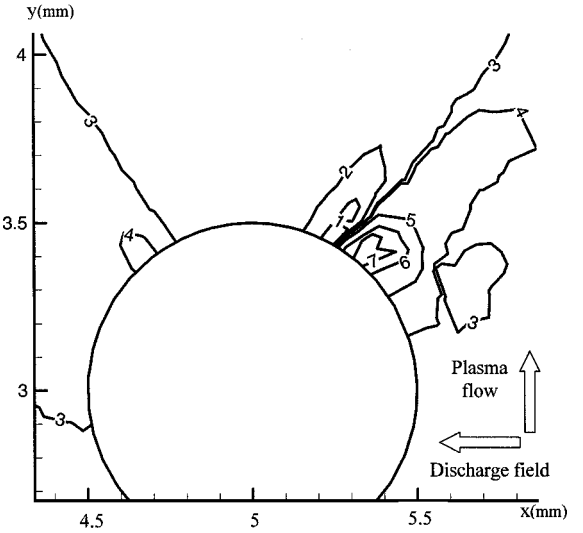

Fig. 7 Contour distribution of the rate of recombination minus the rate of ionization ($\times 10^{-21}$ cm$^{-3} \cdot$ s^{-1}): 1, – 2.5; 2, – 1.0; 3, 0; 4, 0.2; 5, 1.5; 6, 4.2; and 7, 6.

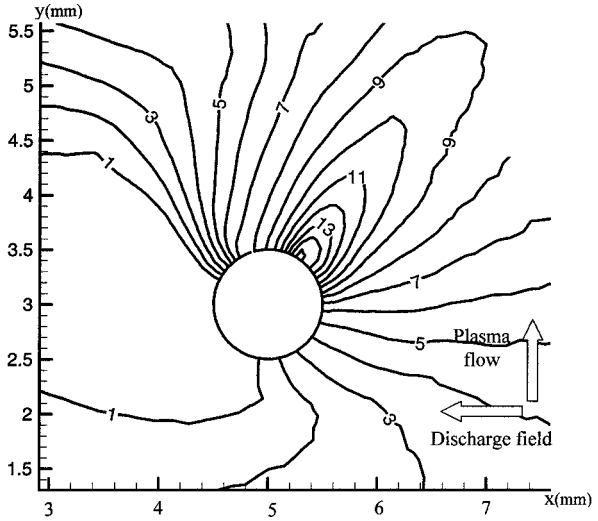

Fig. 8 Distribution of plasma density ($\times 10^{-13}$ cm^{-3}): 1, 1; 3, 1.75; 5, 3.1; 7, 5.5; 9, 10; 11, 17; 13, 30; and 15, 53.

experiments: the probe radius $R = 0.05$ cm, $E_0 = 200$ V/cm, the probe voltage was -40 V, the initial plasma flow parameters were $T_{g0} = 700$ K, $M_0 = 1.1$, $n_{i0} = 10^{13}$ cm^{-3}, $p_{g0} = 43$ torr, and $T_{e0} = 1.9$ eV. Underindicated values of data in a diffusion of ions and electronic thermal conduction are inessential; the appropriate members are excluded from the set of equations.

The gas parameter distributions are typical for the transonic gas flow over a cylinder (see Fig. 5). One can see a remote weak shock wave, unstable vortices behind the body, shock waves near the rear surface of the cylinder, etc. It is important for the following discussion that zones of gas rarefication are formed near the cylinder lateral surface, where the gas density falls more than a factor of two.

The electric field distribution (Fig. 6) is not far from that without the plasma flow, although it is somewhat disturbed in the region of maximal plasma density. Because of the presence of the probe, the electric field is enhanced on one side of the probe and falls to zero on the other side. The ratio E/n_g (which defines heating of the electron gas) is considerably enhanced in one of the two zones of gas rarefaction (on the side where the field intensity is higher). That results in a considerable local growth in the electron temperature and in the ionization rate (Fig. 7). Plasma density in this zone grows dramatically (up to about 50 times in comparison with the unperturbed plasma density). The dense plasma passes through the rear shock wave, where the gas and plasma density become more than twice as high. That gives rise to the recombination rate and fall of the rate of ionization, and, thus, returns the plasma density to the initial value. The resulting region of enhanced plasma density looks like a bias torch (see Fig. 8). As this region contacts the probe surface, the additional ionization affects the total probe current (it is enhanced by a factor of about five).

We do not know any work that describes such a combined effect of the flow density distribution and the discharge field on the plasma density near a probe. This can significantly change the probe voltage–current characteristic, as well as limit the area of applicability of the plasma probe diagnostics, unless the perturbation can be quantified by some special experiment or by calculation. However, our analysis has shown that the area of the probe diagnostics applicability can be expanded by 1) use of a probe with small radius and 2) application of an isolating shell on the part of the probe surface that is in contact with the dense plasma.

Analytical Formulas for Cylindrical Probe in High-Speed Plasma Flow and Intensive Electric Field

There have been no methods of inferring of plasma parameters from the probe voltage–current characteristic under the conditions typical in the plasma aerodynamic experiments (high electric field $E_0 \geq 100$ V/cm, supersonic airflow $M_0 > 1$, high density gas $\rho_g = 10^{-4}$–10^{-3} g/cm^3, high plasma density $n_e \sim 10^{13}$ cm^{-3}, etc.). Our study has shown that, if the effect of extra ionization near the probe is negligible, such an inference is possible. To do so, one needs analytical formulas that express plasma parameters via parameters of the probe voltage–current characteristic. The analysis was based on the equations of the preceding model of the flowing plasma–probe interaction.

The plasma perturbation zone around an electric probe can be divided into three main regions.[1] The space-charge region (debye sheath) adjoins to a probe directly. In this region, it is impossible to neglect separation of charges, that is, the solution of the Poisson equation is necessary. The sheath width depends on the value of debye radius r_d and also on the value of applied voltage.

The quasi-neutral layer is located farther from the probe (diffusion region), where charge separation is small, the Poisson equation is superfluous, and charge transfer by ambipolar diffusion is essential. The thickness of this region depends on the magnitude of the electrical Reynold's number $ReSc_i = v_g R/D_i$, where D_i is an ion diffusion coefficient.

Behind the diffusion region there is the layer of quasi-neutral nonviscous flow (drift region) with the thickness of about a probe radius, in which the drift of the charge particles in the electrical field is the main process of current collection. In the considered case, this field is formed not by the probe bias voltage (classical case[1]) but by the external (discharge) field interacting to a probe one.

Because the experiments were conducted with a double probe, the probe potential is negative relative to the space (plasma) potential and differs from the floating probe potential weakly. Under these conditions, the debye sheath together with the diffusion layer are thin in comparison with the probe radius. However, the diffusion region width is comparable with that of the debye sheath: $ReSc_i r_d/R \gg 1$; therefore,[2] the main part of the potential falls in the drift region. Thereby, the main mechanism of probe current collection is the drift of charge particles in an external field interacting with the field of a probe.

Note that the well-known effect of an ion current saturation,[2] defined by a diffusion current of ions in the region of the thin debye sheath, is realized in the opposite case: $ReSc_i r_d/R \ll 1$.

We consider the limiting case, when the most of the potential falls in the quasi-neutral plasma, that is, the falls of potential across the diffusion layer and debye sheath may be neglected. This case is new: Practically all of the work on probe diagnostics[1,2,4] analyzes either the debye sheath or the diffusion layer. In Ref. 3 voltage–current characteristics defined with electron drift processes are analyzed.

Consider the ion transport processes in the drift area and the resulting voltage–current characteristic. The electric field $\boldsymbol{E}$ distribution in the vicinity of a sufficiently long ($L/R \gg 1$) cylindrical probe with a voltage V_p in the presence of an external (discharge) electric field $\boldsymbol{E}_0$ can be expressed as[3]

$$\mathbf{E}(\boldsymbol{r}) = \boldsymbol{E}_0(1 - R^2/r^2) + \boldsymbol{r}^0 2(R^2/r^2)\left(\boldsymbol{E}_0 \boldsymbol{r}^0\right) + \boldsymbol{r}^0 V_p/[r\ell n(L/R)] \tag{8}$$

where $\boldsymbol{r}^0$ is a radial vector with unity length. The field component normal to the surface E_n in the interface of the drift area and the diffusion layer $r = r_a$:

$$E_n(\psi) = (\boldsymbol{E}\boldsymbol{r}^0) = E_0 \cos\psi\left[1 + R^2\Big/(R + r_a)^2\right] + Vp/[(R + r_a)\ell n(L/R)] \tag{9}$$

in our case $r_a \ll R$ this interface practically coincides with the probe surface, and

$$E_n(\psi) \approx 2E_0 \cos\psi + V_p/[R\ell n(L/R)] \tag{10}$$

The drift current of positive ions through a part A^+ of the probe surface, on which the electric field is directed from the plasma, is

$$I^+ = -\int en_i \mu_i E_n \, \mathrm{d}A^+ \tag{11}$$

and A^+ can correspond to the entire surface. It is also possible that there is a part A^- of the probe surface where the electric field is oppositely directed. The electron current through A^- is

$$I = \int en_e \mu_e E_n \, \mathrm{d}A^- \tag{12}$$

Since $\mu_e \gg \mu_i \approx \mu_-$, one can neglect the yield of negative ions. It also means that $A^- \ll A^+$: Otherwise, the ion current would be negligible, for example, for zero total probe current $I = I^+ - I^-$, it is necessary to charge the probe so that the area A^- of the surface where $E_n > 0$ would be negligible. It means that in the area A^- the field is practically a zero. In accordance with Eq. (10), the threshold field distribution with zero area A^- corresponds to the probe potential:

$$V_p^0 = -2E_0[R\ell n(L/R)] \tag{13}$$

Note that, on the opposite side of the probe, the field is then maximal and equal to $\approx 4E_0$. For probe diagnostics of dense plasmas with high electric field E_0, the probe voltage should be about V_p^0: $V_p = V_p^0 + \Delta V_p$, $|\Delta V_p| \ll |V_p^0|$. The normal field distribution is then

$$E_n \approx 2E_0 \cos\psi + 2E_0 + \Delta V_p/[R\ell n(L/R)] \approx 2E_0(\cos\psi + 1) \tag{14}$$

Let the cylindrical probe axis z be positioned normally to $\boldsymbol{E}_0$ and $\boldsymbol{v}_g$, $z \perp \boldsymbol{E}_0 \perp \boldsymbol{v}_g$. The plasma flow separates in the fore point $\psi = \pi/2$ of the cross section of the probe cylinder, where $E_n \approx -2E_0$, and rejoins in the opposite side, where $\psi = 3\pi/2$, and again $E_n \approx -2E_0$ (here the negative normal field corresponds to negative probe voltage). One-half of plasma flows through the region near the probe with a considerably enhanced electric field (with a maximum at $\psi = \pi$). The corresponding yield to the total ion current is

$$I_{i1} = LR \int_{\pi/2}^{3\pi/2} en_{i1}(\psi)\mu_i E_n \, d\psi \approx 2(\pi + 2)RL\, en_{i\infty}\mu_i E_0 \quad (15)$$

The other half of plasma flows in a relatively attenuated field, with a minimal point about zero, $|E_n| = |\Delta V_p/[R\ell_n(L/R)]| \ll |E_0|$, near $\psi = 0$. If $\Delta V_p < 0$, this part of probe surface also collects only ions,

$$I_{i2} = RL \int_{-\pi/2}^{\pi/2} en_{i2}\mu_i E_n \, d\psi = 2(\pi - 2)RL\, en_{i\infty}\mu_i E_0 \quad (16)$$

Note that it is $(\pi + 2)(\pi - 2)$ times less than the ion current on the opposite side. If $\Delta V_p > 0$, the total current on this side of the probe is composed of ion and electron components. The ion current term

$$I_{i2} = RL \int_{-\pi/2}^{\psi^-} en_{i2}\mu_i E_n \, d\psi RL + \int_{\psi^+}^{\pi/2} en_{i2}\mu_i E_n \, d\psi$$

$$\psi_\pm = \pm\{\Delta V_p/[2E_0 R\ell_n(L/R)]\}^{\frac{1}{2}} \quad (17)$$

where ψ_+ and ψ_- are the zero field points, $E_n(\psi_+) = E_n(\psi_-) = 0$. If $|\psi_\pm| \ll \pi$, then again one gets

$$I_{i2} = RL \int_{-\pi/2}^{\pi/2} en_{i2}\mu_i E_n \, d\psi \approx 2(\pi - 2)RL\, en_{i\infty}\mu_i E_0 \quad (18)$$

The electron term is

$$I_e = RL \int_{\psi^+}^{\psi^-} en_{e2}\mu_e E_n \, d\psi \quad (19)$$

If $|\psi_\pm \ll \pi$, then the field between ψ_- and ψ_+ is $E_n(\psi) \approx 2E_0\,\psi^2 + \Delta V_p/[R\ell_n(L/R)]$. Integration yields the formula[3]

$$I_e = RL\, n_{i\infty} e\mu_e \left(2^{\frac{3}{2}}/3\right)\{\Delta V_p/[R\ell_n(L/R)]\}^{\frac{3}{2}}/E_0^{\frac{1}{2}} \quad (20)$$

The probe extra voltage $\Delta V_p = \Delta V_{p0}$ providing zero total current can be obtained from the equality of ion and electron currents, $I_e = I_{i1} + I_{i2}$, as

$$\Delta V_{p0} = R\ell_n(L/R)\left(3\pi 2^{\frac{1}{2}}\mu_i/\mu_e\right)^{\frac{2}{3}} E_0 \quad (21)$$

Thus, the probe voltage–current characteristic $I = I(\Delta V_p)$ is the following: At $\Delta V_p \le 0$, the probe current $I = -I_i$; here, $I_i \equiv (I_{i1} + I_{i2})$ is the ion saturation current. Under the assumptions listed earlier it does not depend on ΔV_p and is in direct proportion to the discharge field E_0 and to the plasma degree of ionization near the probe $x = n_i/n_{\text{mol}}$. In this region, I is practically independent of voltage ΔV_p. At $\Delta V_p > 0$, the positive electron current $I_e \sim \Delta V_p^{2/3}$ is added to the ion voltage-independent term. The total current passes the $I = 0$ point at $\Delta V_p = \Delta V_{p0}$. For example, for $E_0 = 1$ kV/cm and $R = 0.05$ cm, $L = 0.5$ cm, $T_e = 2$ eV, $T_g = 300$ K, and the voltage $\Delta V_{p0} \approx 6$ V. For comparison, the corresponding probe voltage level $V_{p0} \approx -180$ V.

Consider the possibility of probe diagnostics of plasma parameters. One can get two characteristic values from an experimental voltage–current characteristic of such a type: The ion saturation current I_i and the voltage ΔV_{p0}, which provides a zero total current. It is useful to express these values via arbitrary plasma parameters $n_{i\infty}, n_g, E_0, T_e$, and T_g, and probe sizes R and L. For weakly ionized plasma of a given composition, the electron and ion mobilities are in an inverse proportion to n_g; in a broad range of parameters, μ_i depends primarily on T_g and μ_e depends on T_e. For example, for the air plasma $\mu_i \approx \mu_i^0 T_g^{1/3}/n_g$, $\mu_i^0 = \text{const}$, $\mu_e \approx \mu_e^0/(T_e n_g)$, and $\mu_e^0 = \text{const}$. Substitution of these approximations into the formulas for I_{i1}, I_{i2}, and ΔV_{p0} gives

$$I_i \approx \frac{4\pi\mu_i^0 RLen_{i\infty}}{n_g T_g^{\frac{1}{3}} E_0}$$

$$\Delta V_{p0} \approx R\ell_n\left(\frac{L}{R}\right)\left[3\pi 2^{\frac{1}{2}}\left(\frac{\mu_i^0}{\mu_e^0}\right)T_g^{\frac{1}{3}} T_{e\infty}\right]^{\frac{2}{3}} E_0 \quad (22)$$

which makes it possible to express the unperturbed degree of ionization $x_\infty = n_{i\infty}/n_g$ and the unperturbed local discharge electric field E_0 via the parameters of a voltage–current characteristic I_i and ΔV_{p0} as

$$E_0 = \Delta V_{p0}(R)/\left\{R\ell_n(L/R)\left[3\pi 2^{\frac{1}{2}}\left(\mu_i^0/\mu_e^0\right)T_g^{\frac{1}{3}} T_{e\infty}\right]^{\frac{2}{3}}\right\} \quad (23)$$

$$x_\infty = I_i(R)/\left[4\pi\mu_i^0 eRLT_g^{\frac{1}{3}} E_0\right] \quad (24)$$

The dependencies of E_0 and x_∞ on the unperturbed gas and electron temperatures from these expressions are rather weak: One can get from Eqs. (23) and (24) that $E_0 \sim T_g^{-1/3}$ and $x_\infty \sim T_g^{-1/9} T_{e\infty}^{2/3}$. It means that an uncertainty of estimation of the temperatures does not result in considerable errors in the determination of E_0 and x_∞.

Determination of Plasma Density from Probe Voltage–Current Characteristic

A typical voltage–current characteristic of the double probe in the dc plasma discharge in supersonic airflow is presented in Fig. 9. No smoothing of the experimental signal shown in Fig. 3 has been done. The high dispersion of the experimental points manifests a very high level of fluctuation of the discharge voltage and a lack of homogeneity in the plasma jet parameters. The probe signal can be smoothed either by a special improvement of the scheme, or by the corresponding data processing with the computer. The measured voltage–current probe characteristics show two typical parts of ion current saturation and a very narrow transition region.

The value of ΔV_{p0} in the current experiment was too small, and the level of noise was very high. Therefore, the accuracy of definition of ΔV_{p0} in this specific case was poor. Thus, the simultaneous definition of $n_{i\infty}$ and E_0 from the probe characteristic was impossible.

The discharge electric field E_0 was measured independently from the probe characteristic, as the value of the difference of floating potentials of two independent probes in longitudinal and transversal directions to a flow. These signals were fixed on the storage oscilloscope and averaged on the period of oscillations. The resulting field was determined as the vector sum of longitudinal and transversal componens of electric field.

The values of gas temperature and gas density are necessary for definition of ion density based on Eq. (24). The gas temperature was measured by spectral methods over relative intensities of lines of the

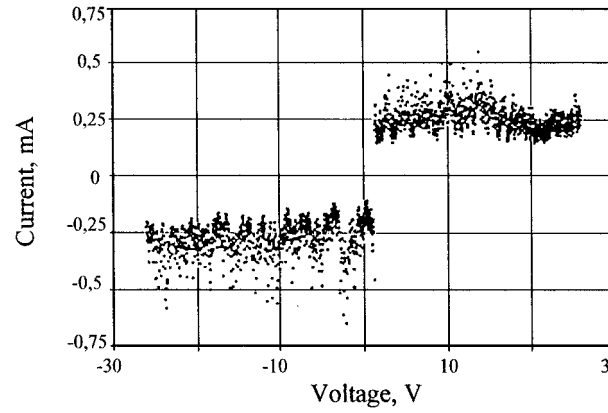

Fig. 9 Voltage–current characteristic of the double probe in the supersonic plasma of dc discharge: probe $R = 0.2$ mm, $p = 40$ torr, $I = 0.2$ A, $M = 2$, and cathode plasma channel.

rotational structure of the band (0; 2) with the quantum wave length $\lambda = 380.5$ nm of the second positive system of nitrogen molecule and of the band (0; 0) with quantum wave length $\lambda = 388.3$ nm of the CN molecule.

As the average gas temperature as a function of the longitudinal coordinate of the discharge was measured, the average gas density was determined from the equation of state of the ideal perfect gas. The discharge pressure was taken to be equal to the nearby gas flow pressure; the latter results from our numerical simulation[9,10] of the discharge.

Spectral Method of Measurement of Electron Density

The electron density in the discharge plasma in the supersonic airflow was also determined by the spectral method based on the Stark broadening of a spectral line with by use of

$$n_e = C(n_e, T_e)(\Delta\lambda)^{\frac{3}{2}} \tag{25}$$

where $\Delta\lambda$ is the linewidth and $C(n_e, T_e)$ is the Stark constant, which is weakly dependent on n_e and T_e. This expression can be presented graphically as $\ln n_e = f(\ln \Delta\lambda)$. The H_β line with $\lambda = 4861$ Å has proved to be the most convenient for plasma density diagnostics. That is due to a number of factors. Actually, this line is located in the spectral area, where usual radiation sensors have a high sensitivity. At plasma density $n_e \geq 10^{13}$ cm^{-3}, the H_β line's broadening is large, and it is possible to measure its width with the help of the usual spectral devices. The accuracy of theoretical determination of the H_β linewidth is better than 5%, whereas it is about 10% for the other lines of hydrogen. The H_β line corresponds to the transition between rather low energy levels. Therefore, as a rule, it is sufficiently bright in the plasma, even if the hydrogen is present as a small impurity.

To make such a type of diagnostics possible, hydrogen was added in a small amount into a supersonic airflow. The Doppler effect and the apparatus function of the spectral device bring an appreciable contribution in the profile of the registered line. Under the conditions of the experiments, the gas temperature is about 1000 K, which corresponds to the H_β line broadening $\Delta\lambda = 0.1$ Å. The dependence of the apparatus function of the spectral device on the width of an entrance slot was determined with registration of the width of an He–Ne laser line ($\lambda = 6328$ Å). At electron density $n_e \geq 10^{13}$ cm^{-3}, the Stark broadening of hydrogen lines is the most effective mechanism of line broadening.

Plasma Density Measurement by a Microwave Interferometer

Independent measurements of the electron density by a microwave (MW) interferometer with dielectric antennas[11] were made. The wavelength λ was 8 mm, which corresponds to an angular frequency $\omega = 2.3 \times 10^{11}$ s^{-1} and to critical electron density $n_e = 1.65 \times 10^{13}$ cm^{-3}. The model of a plane layer in an approximation of geometric optics was used. Then, the simple relation between electron density, the thickness of the plasma layer d, and phase shift $\Delta\varphi$ can be applied:

$$\Delta\varphi = (2\pi d/\lambda)\left(1 - \sqrt{1 - n/n_e}\right) \tag{26}$$

if the following conditions are realized: $\nu < \omega$ and $D/\lambda \geq 3$. Here ν is the frequency of collisions of electrons with heavy particles and D is the plasma size in the direction perpendicular to the propagation of the MW probing wave. These conditions are realized in our experiments. The accuracy of MW measurements is not very high because of a strong inhomogeneity of the plasma in the direction perpendicular to propagation of the MW sounding wave. Application of the cutoff method seems to be more effective. It can be applied at high discharge currents at the distance from the nozzle where the mixing of plasma with the air is essential. This situation is realized in the PP discharge.

Some results of a comparison of the three diagnostic methods for the dc and the PP discharge plasmas in supersonic airflow are shown in Fig. 10. The probe and spectral signals are received from an area of one of the discharge channels at a distance $z = 30$–40 mm from the electrodes, whereas the MW signal is obtained for $z = 40$–50 mm.

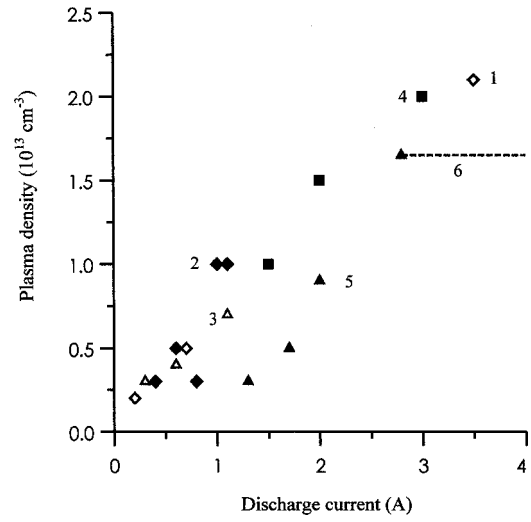

Fig. 10 Electron density measured by different methods over the discharge current at $p = 40$ torr: 1, probe $R = 0.2$ mm; 2, probe $R = 0.5$ mm; 3, microwave interferometer; 4, spectral method; 5, microwave interferometer in the pulsed periodic discharge; and 6, cutoff level.

The accuracy of ion density definition based on the probe characteristic is determined mainly by the accuracy of determinations of gas density and discharge electric field. It was of the order of 50% in our experiments. The error of spectral measurement of electron density was about 20%.

One can see that the three independent methods yield reasonably close values of the electron density $n_e \sim 10^{13}$ cm^{-3}. Note that the MW method shows lower limits and the spectroscopic method upper limits of n_e. This result confirms the validity of the developed probe method.

Probe Measurements in Plasma Aerodynamic Experiments

The developed automatic probe systems were applied to measure electron density at discharges in a wind tunnel. These experiments[12] were carried out in the TsAGI (Central Aerohydrodynamic Institute, Zhukovsky, Russia) wind tunnel ($M = 2$) with a conic model 168 mm in diam at static pressure $P = 200$ torr. A PP longitudinal discharge was formed around the model between its spike and eight sectioned electrodes situated on its lateral surface. The discharge parameters were the power supply frequency 40 Hz, the discharge current amplitude 100 A, and the average input power 1.6 kW. A very high level of noise is characteristic of such a discharge. The double probe was positioned between the anode and the cathode with a 4-mm separation from the model's surface. The probe measurement cycles were synchronized with the discharge pulses. The ion saturation current measured by the circuit with optical waveguide did not exceed 1 mA, which corresponds to the plasma density no more than 10^{13} cm^{-3}.

At the same time, the use of the circuit with the optocoupler, in which the exchange of signals with the computer was carried out through a standard computer cable, results in a halt of the computer because of the high level of noise. This phenomenon occurs despite of its feeding through a uninterrupted power supply (back-UPS). Thus, only an optical transfer of the signal to and from the computer is efficient. In addition, it is necessary to use the power supply of the computer through a back-UPS and to screen all of the cables including those for keyboard and mouse.

Conclusions

In this paper, the method of double electrostatic continuum probes was used for the measurement of plasma density in a transversal dc discharge in a supersonic airflow.

A very high and oscillating plasma floating potential relative to the ground potential (about some kilovolts) required application of a PC-controlled probe circuit with an optogalvanic isolation between a probe and recording equipment.

A very high electric field in the discharge plasma required also the study of a new case of the probe voltage–current characteristic when probe current collection is determined not only by the probe bias but also by the discharge electric field.

We have considered a limiting case, when the drift of ions in the electric field is the main mechanism of probe current collection. The saturation of the probe current appears on the voltage–current characteristic of the double probe in this limiting case. Analytical expressions for the magnitude of ion saturation current and potential of saturation have been obtained.

The probe disturbs both the distribution of the dc discharge electrical field and the gasdynamical structure of the supersonic flow. Our numerical simulation has shown the possibility of a combined effect of these disturbances, which limits the area of application of the probe method.

The values of the plasma density as derived from probe voltage–current characteristics based on the developed theory differ from plasma density measurements by a microwave interferometer and the method based on the Stark broadening of a spectral line within the factor of 2.

Acknowledgment

This work was supported by Boeing North American, Inc., Contract L8CY-399927-4-861.

References

[1]Chung, P., Talbot, L., and Touryan, K., *Electric Probes in Stationary and Flowing Plasmas: Theory and Application*, Springer-Verlag, New York, 1975, Chap. 3.

[2]Benilov, M. S., "Theory of Electrical Probes in Flows of High Pressure Weakly Ionized Plasma (a Review)," *High Temperature*, Vol. 26, No. 5, 1988, pp. 780–793.

[3]Akishev, Y. S., and Napartovich, A. N., "Probe Measurements in Glow Discharge at High Pressures," *Doklady Physics*, Vol. 242, No. 4, 1978, pp. 812-815 (in Russian).

[4]Benilov, M. S., "Weakly Ionized Gas Flow in Hypersonic Viscous Shock Layer," *Hypersonic Aerodynamics with Injection*, Moscow State Univ., Moscow, 1979, pp. 167–173 (in Russian).

[5]Dvinin, S. A., Ershov, A. P., Timofeev, I. B., Chernikov, V. A., and Shibkov, V. M., "Features of the Transversal Gas Discharge in a Supersonic Gas Flow," *The 2nd Workshop on Magneto-Plasma Aerodynamics in Aerospace Applications*, Inst. of High Temperatures of RAS (IVTAN), Russian Academy of Sciences, Moscow, 2000, pp. 169–174.

[6]Osipov, Y. I., "New Method of a Probe Characteristic Measurement," *Technical Physics*, Vol. 44, No. 2, 1974, pp. 474–476 (in Russian).

[7]Protasov, Y. S., and Chuvashev, S. N., *Physical Electronics of Gas Discharge Devices. Plasma Electronics*, Vysshaya Shkola, Moscow, 1993, pp. 122–240 (in Russian).

[8]Ardelyan, N. V., Kosmachevskij, K. V., and Chuvashev, S. N., "Computer Simulation and Theoretical Studies of Radiating Plasmadynamic Discharge," *Radiating Plasma Dynamics*, Energoatomizdat, Moscow, 1991, pp. 191–249 (in Russian).

[9]Chuvashev, S. N., Ershov, A. P., Klimov, A. I., Leonov, S. B., Shibkov, V. M., and Timofeev I. B., "Flow Around Body and Characteristics of AC/DC Discharges in Plasma Aerodynamic Experiment," *Proceedings of the 2nd Weakly Ionized Gases Workshop, AIAA 8th International Space Planes and Hypersonic Systems and Technologies Conference*, AIAA, Reston, VA, 1998, pp. 59– 67.

[10]Georgievsky, P. Y., Gromov, V. G., Ershov, A. P., Levin, V. A., Timofeev, I. B., Chernikov, A. V., Chernikov, V. A., and Shibkov, V. M., "Gas Discharge in Supersonic Flow," *2nd Workshop on Magneto-Plasma Aerodynamics in Aerospace Applications*, Inst. of High Temperatures of RAS (IVTAN), Russian Academy of Sciences, Moscow, 2000, pp. 143–149.

[11]Anders, A., Ershov, A. P., and Isaev, K., "Study of an Underexpanded Plasma Jet II. Diagnostics with Microwaves," *Contributions to Plasma Physics*, Vol. 28, No. 6, 1988, pp. 537–542.

[12]Beaulieu, W., Bytyurin, V., Klimov, A., Leonov, S., Pashina, A., and Timofeev, B., "Plasma Aerodynamic WT Tests with $\frac{1}{6}$ Scale Model of Nose Part of F-15," AIAA Paper 99-4825, 1999.

R. P. Lucht
Associate Editor